# Regular Article

## LYMPHOID NEOPLASIA

# Astatine-211 conjugated to an anti-CD20 monoclonal antibody eradicates disseminated B-cell lymphoma in a mouse model

Damian J. Green,[1,2] Mazyar Shadman,[1,2] Jon C. Jones,[1] Shani L. Frayo,[1] Aimee L. Kenoyer,[1] Mark D. Hylarides,[1] Donald K. Hamlin,[3] D. Scott Wilbur,[3] Ethan R. Balkan,[3] Yukang Lin,[1] Brian W. Miller,[4] Sofia H. L. Frost,[1] Ajay K. Gopal,[1,2] Johnnie J. Orozco,[1,2] Theodore A. Gooley,[1] Kelly L. Laird,[1] Brian G. Till,[1,2] Tom Bäck,[5] Brenda M. Sandmaier,[1,2] John M. Pagel,[1,2] and Oliver W. Press[1,2]

[1]Clinical Research Division, Fred Hutchinson Cancer Research Center, Seattle, WA; Departments of [2]Medicine and [3]Radiation Oncology, University of Washington, Seattle, WA; [4]Pacific Northwest National Laboratory, Richland, WA; and [5]Department of Radiation Physics, University of Gothenberg, Gothenberg, Sweden

---

## Key Points

- α-Emitting radionuclides have the potential to overcome treatment-resistant lymphoma cell clones that evade other forms of therapy.
- [211]At-labeled anti-CD20 monoclonal antibody eradicates lymphoma in a mouse minimal residual disease model.

α-Emitting radionuclides deposit a large amount of energy within a few cell diameters and may be particularly effective for radioimmunotherapy targeting minimal residual disease (MRD). To evaluate this hypothesis, [211]At-labeled 1F5 monoclonal antibody (mAb) (anti-CD20) was studied in both bulky lymphoma tumor xenograft and MRD animal models. Superior treatment responses to [211]At-labeled 1F5 mAb were evident in the MRD setting. Lymphoma xenograft tumor-bearing animals treated with doses of up to 48 μCi of [211]At-labeled anti-CD20 mAb ([[211]At] 1F5-B10) experienced modest responses (0% cures but two- to threefold prolongation of survival compared with negative controls). In contrast, 70% of animals in the MRD lymphoma model demonstrated complete eradication of disease when treated with [211]At-B10-1F5 at a radiation dose that was less than one-third (15 μCi) of the highest dose given to xenograft animals. Tumor progression among untreated control animals in both models was uniformly lethal. After 130 days, no significant renal or hepatic toxicity was observed in the cured animals receiving 15 μCi of [[211]At]1F5-B10. These findings suggest that α-emitters are highly efficacious in MRD settings, where isolated cells and small tumor clusters prevail. (Blood. 2015;125(13):2111-2119)

## Introduction

Treatment regimens incorporating monoclonal antibodies (mAbs) targeting CD20 have improved response rates and prolonged progression-free survival (PFS) for patients with non-Hodgkin lymphoma (NHL). Unfortunately, the benefits of conventional immunochemotherapy and radiation therapy are only temporary in the setting of advanced-stage indolent or mantle cell NHL, and relapse is universal. Recently, small-molecule inhibitors of Bruton tyrosine kinase have demonstrated efficacy in relapsed mantle cell lymphoma (MCL)[1]; however, conventional chemotherapy has not been curative, and durations of response have been short.[2,3] Minimal residual disease (MRD) following therapy consists of microscopic foci of treatment-insensitive tumor cells, the presence of which is predictive of frank relapse. Induction regimens that eliminate MRD can significantly improve the duration of response to treatment.[4-6] In MCL, MRD status after autologous stem cell transplant (ASCT) is predictive of PFS, event-free survival, and overall survival,[7] and among MCL patients achieving a molecular remission after ASCT, a median PFS of 92 months has been reported, as compared with 21 months in MRD-positive individuals (P < .001).[8]

Lymphomas are exquisitely sensitive to radiation, and the directed delivery of radionuclides to tumor cells through radioimmunotherapy (RIT) targeting CD20 has been shown to effectively improve response

rates among patients with advanced-stage indolent and mantle cell NHL.[9-18] These responses may reflect the reduction or even elimination of MRD. Toxicities with myeloablative doses of β-particle RIT remain significant, however, and ~50% of patients ultimately relapse.[19] Not surprisingly, higher doses of absorbed radiation to tumors delivered by RIT correlate with a reduced risk of disease recurrence, but dose-limiting toxicities prevent escalation.[10,20]

The selection of β-emitting radionuclides ^{131}I and ^{90}Y to potentiate CD20 antibodies in the "first generation" of RIT agents was based on the relative availability, high-energy emissions, favorable half-lives, and radiochemical stability of the radiolabel. The long path lengths of their β-emissions, however, result in the delivery of a large fraction of their energy to nontarget sites, with dose-limiting myelosuppression at conventional doses[21,22] and cardiopulmonary toxicity with the higher myeloablative doses required for ASCT conditioning.[9,10,23,24] In addition, the low-linear energy transfer of β-particles may result in suboptimal killing of tumor cells, ultimately leading to relapse in most patients.

α-Emitting radionuclides have recently become more broadly available and advances in radiochemistry have enabled the production of a bifunctional closo-decaborate(2-) (B10-NCS) radiolabeling platform capable of providing critical stability to α-particle–labeled

---

2111

biomolecules.[25] The α-emitter [211]At deposits a very large amount of energy (~100 keV/μm) within a few cell diameters (50-90 μm), resulting in irreparable double-strand DNA breaks that overwhelm cellular repair mechanisms. The combination of high-energy emissions and short path length confer a unique capacity for α-emitters to kill individual targeted cells with minimal radiation damage to surrounding tissues and offers a theoretical advantage over β-emitters. The physical characteristics of α-emitters coupled with new opportunities to harness their potential, provide a compelling rationale for exploring α-emitter RIT designed to selectively and comprehensively eliminate MRD. Here, we report results from studies using [211]At-labeled anti-CD20 mAb 1F5-B10 in murine subcutaneous tumor xenograft and disseminated lymphoma models.

# Methods

## Cell lines

The human Ramos (Burkitt lymphoma) and Jurkat (T lymphoblastic lymphoma) cell lines were obtained from American Type Culture Collection (Bethesda, MD); Granta-519 (MCL) was obtained from Deutsche Sammlung von Mikroorganismen und Zellkulturen (Braunschweig, Germany). Cell viability exceeded 99% by trypan blue exclusion for cells used in these experiments. For in vitro studies, cells were maintained in log-phase growth in RPMI 1640 supplemented with 10% fetal bovine serum, 50 U/mL penicillin G, and 50 μg/mL streptomycin sulfate. Following 2 passages, cells were frozen and stored in liquid nitrogen for future use. For all xenograft studies, a fresh vial of frozen cells was thawed and grown in culture for 7 to 14 days before implantation. The Granta 519 firefly luciferase cell line (Granta-519$^{Luc}$) was generated by retroviral transduction to stably express firefly luciferase for in vivo bioluminescent imaging (BLI; detailed in supplemental Methods available on the *Blood* Web site).

## Mice

Female FoxN1Nu athymic nude mice (Harlan Sprague-Dawley) and NOD. BCB17-Prkdc$^{scid}$/J mice (nonobese diabetic severe combined immunodeficiency [NOD/SCID], Fred Hutchinson Cancer Research Center [FHCRC] colony) were housed, maintained, and killed following protocols approved by the FHCRC Institutional Animal Care and Use Committee.

## Antibodies

The 1F5 hybridoma cell line expressing the murine immunoglobulin G$_{2a}$ anti-human CD20 antibody was a gift from Clay Siegall (Seattle Genetics, Seattle, WA). The antibody was produced from the hybridoma using a hollow-fiber bioreactor system in the mAb production facility at FHCRC. The HB8181 hybridoma (immunoglobulin G$_{2a}$ isotype control) was purchased from American Type Culture Collection, and antibody was produced in the peritoneal ascites of pristane-primed BALB/c mice. In all biodistribution and therapy experiments, mice were coinjected with 400 μg of HB8181 to block nonspecific binding of the 1F5 to Fc receptors.

## Bifunctional decaborate (B10-NCS) reagent and conjugation to 1F5 and HB8181

The amine-reactive bifunctional labeling reagent, isothiocyanato-phenethyl-ureido-*closo*-decaborate(2-) (B10-NCS) (supplemental Figure 1), was prepared as previously reported. Conjugation of B10-NCS to the antibodies was performed using the method of Wilbur.[26,27]

## Radiolabeling

For biodistribution studies, 1F5-B10 was radioiodinated with Na[125]I (Perkin Elmer, Boston, MA) by the chloramine T method as previously described.[26] Radiochemical purity was typically greater than 99% as determined by instant thin-layer chromatography, and labeling efficiencies were >70%. [211]At was produced on a Scanditronix MC-50 cyclotron at the University of Washington using methods previously described.[28] 1F5-B10 labeling with [211]At is detailed in supplemental Methods. Labeling reactions yielded an [211]At recovery of 78% to 79% ([[211]At]1F5-B10) and 83% to 86% ([[211]At]HB8181-B10) and protein recovery of 68% to 80% (1F5-B10) and 79% to 83% (HB8181-B10).

## Cell-binding analysis of radiolabeled 1F5-B10

Anti-CD20 (1F5-B10) (20 μg/mL) or nonbinding control (HB8181-B10) (20 μg/mL) was added to Ramos and Jurkat cells (1 × 10$^6$/well) pelleted in 96-well round-bottom plates on ice. Pellets were resuspended in the antibody solution, incubated at 4°C for 45 minutes, and washed and resuspended in 200 μL phosphate-buffered saline. [[211]At]1F5-B10 or [^{125}I]1F5-B10 (20 μg/mL) was added, and cells were incubated at 4°C for 45 min, washed 3 times, and the cell-associated radioactivity was measured in a γ counter.

## Biodistribution studies

Female athymic nude mice were injected subcutaneously in the right flank with Ramos cells (1 × 10$^7$) ~7 days prior to therapy to obtain lymphoma xenografts. Mice were administered anti-asialoGM1 antiserum (200 μL intraperitoneally; WAKO, Richmond, VA) 8 days and 4 days prior to the radiolabeled antibody injection to abrogate natural killer cell activity and prevent spontaneous tumor regressions. Mice with similar-sized, palpable tumors were chosen for the studies. For biodistribution studies, mice were injected IV via the lateral tail vein with 1.4 nmol of radioastatinated mAb (210 μg; 50 μCi). Mice were bled from the retro-orbital venous plexus, killed, and tumors and normal organs (lung, liver, spleen, stomach, kidneys, small intestine, colon, throat, muscle, and tail) were harvested, weighed, and γ counted for [211]At activity 24 hours after the [[211]At] 1F5-B10 injections. The percent-injected dose of [211]At per gram (%ID/g) of blood, tumor, and normal organs was calculated after correcting for background and radioactive decay, using an aliquot of the injectate as a standard. Tumor-to-normal organ ratios of absorbed radioactivity were also calculated. Control groups were injected with radiolabeled isotype-matched, nonbinding control [[211]At]-HB8181-B10.

## α-Camera imaging

A scintillator-based camera dedicated to α-particle detection enabled digital autoradiographic imaging to evaluate the distribution of α-particles in lymphoma xenograft tumors after [[211]At]1F5-B10 (see supplemental Methods).[29,30]

## Subcutaneous lymphoma xenograft therapy studies

Female athymic nude mice were injected subcutaneously in the right flank with Ramos or Granta 519$^{Luc}$ cells (1 × 10$^7$) ~7 days prior to therapy to obtain lymphoma xenografts. When tumors were ~100 mm$^3$ ± 10%, groups of 10 mice each were injected via the tail vein with 210 μg [[211]At] 1F5-B10 labeled with 12, 16, 24, 36, or 48 μCi of [211]At (maximum dose defined by [211]At toxicity reported in a nude mouse model)[31] or nonbinding control. Tumor size and body weight were measured daily following injections. Mice were killed when they experienced weight loss >30% or tumor growth >16 × 16 × 9 mm, per animal health guidelines. Data analysis and graphing were performed using GraphPad Prism 6.0 (La Jolla, CA). To prevent misleading fluctuations in tumor volume graphs and facilitate interpretation of the data, the mean tumor volume for each group was truncated after the first mouse in each group was killed.

## Disseminated lymphoma therapy studies

Female NOD/SCID mice (n = 10/experimental condition) were injected IV with Ramos or Granta519$^{Luc}$ cells (1 × 10$^6$) via the tail vein 2 to 6 days before treatment. Mice in the experimental treatment groups received 115 μg of 1F5 labeled with 7.5, 10, or 15 μCi of [211]At. Control mice received saline, 1F5-B10 (unlabeled), or nonbinding HB8181-B10 antibody labeled with 10 or 15 μCi of [211]At. All mice received infusions of 10 to 15 × 10$^6$ syngeneic donor bone marrow cells without T-cell depletion 2 days after the treatment dose. Mice were followed, and their body weights were measured

**Figure 1. Cell-binding assays evaluating the absolute (counts per minute [cpm]) binding of 1F5-B10 labeled with either $^{211}$At or $^{125}$I with or without unlabeled blocking antibodies using Ramos and Jurkat cells confirm the antigen-specific cell binding of radiolabeled 1F5-B10 conjugates.** (A) [$^{211}$At]1F5-B10 binding to Ramos cells was blocked by preincubation with unlabeled anti-CD20 antibodies (2321.0 ± 475.1 vs 409.0 ± 27.5 CPM; 82% blocking). (B) Similar blocking was also observed when the 1F5-B10 was labeled with $^{125}$I (14 642 ± 3621 vs 679 ± 60.6 CPM; 95% blocking). No difference was seen between the binding of 1F5-B10 antibody to the CD20-negative Jurkat cells in the presence or absence of blocking anti-CD20 antibodies. PBS, phosphate-buffered saline.
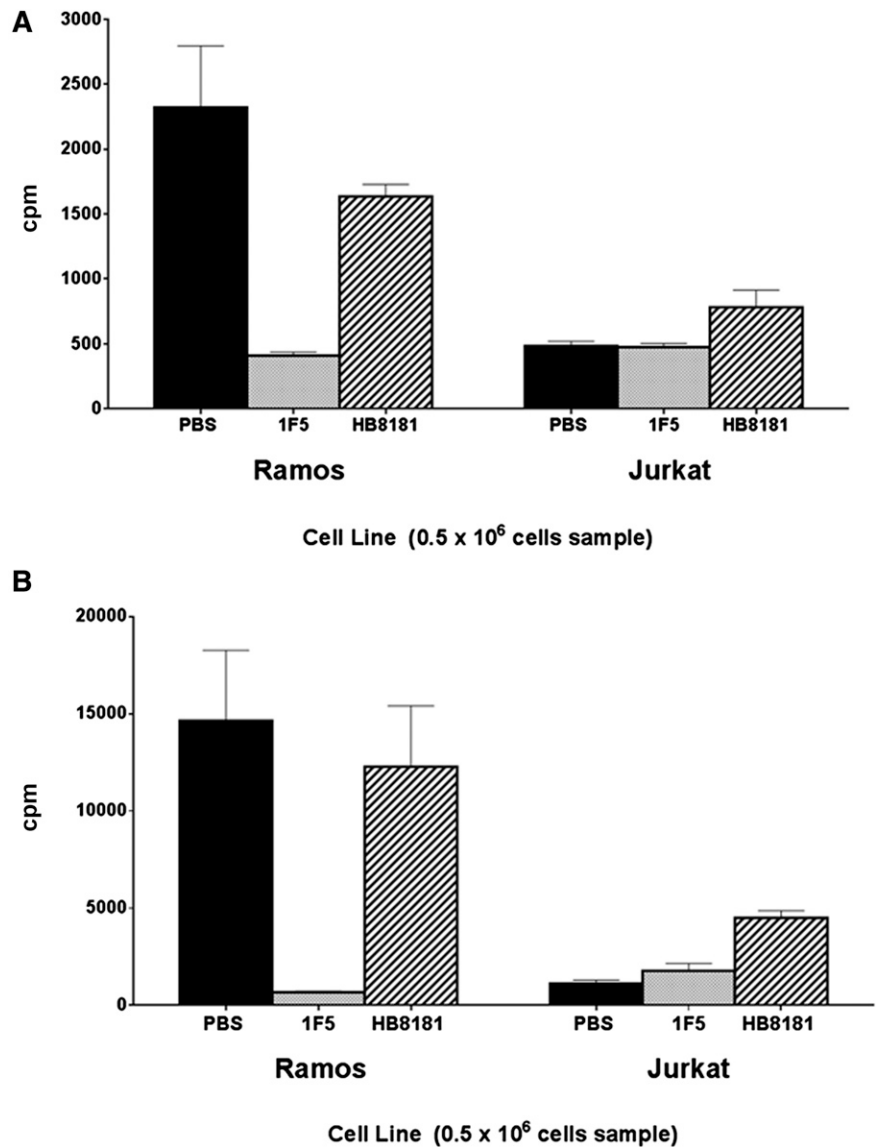
thrice weekly. Mice were killed if they developed hindlimb paralysis, weight loss >30% of the baseline, or if their body condition or activity level deteriorated below acceptable levels established by FHCRC veterinary staff. Based on experience from the pilot studies, supportive care (ie, subcutaneous saline injections to prevent dehydration) was provided daily during the first 10 days after treatment. In some experiments, blood samples from terminal bleeds were obtained to assess blood counts and renal and hepatic function. Mice were monitored throughout the study for lymphoma tumor burden, as measured by in vivo BLI (Granta-519$^{luc}$; detailed in supplemental Methods), and survival (Granta-519$^{luc}$, Ramos).

### Statistical considerations

Differences in lymphoma tumor xenograft volumes were compared by computing the means and standard deviations of each treatment group and employing the Student $t$ test to determine statistical significance. For relatively large differences in tumor volume, 8 to 10 mice per group were projected to provide adequate power to detect statistically significant differences. In the disseminated disease model, tumor burden was calculated based on the mean and standard deviation values measured by total BLI (photons/s), again using the Student $t$ test to determine statistical significance. Only the detection of large differences between treatment groups was considered to be of clinical interest.

## Results

### Cell-binding assays

We measured the binding of 1F5-B10 antibody radiolabeled with either $^{211}$At or $^{125}$I to the CD20-positive human Burkitt lymphoma cell line (Ramos) and CD20-negative T lymphoid tumor cells (Jurkat) to confirm the antigen-specific cell binding of radiolabeled 1F5-B10 constructs. The binding of [$^{211}$At]1F5-B10 to Ramos cells was blocked by preincubation with unlabeled anti-CD20 antibodies (2321.0 ± 475.1 vs 409.0 ± 27.5 CPM; 82% blocking; Figure 1). Similar blocking was also observed when the 1F5-B10 was labeled with $^{125}$I (14 642 ± 3621 vs 679 ± 60.6 CPM; 95% blocking). As expected, there was no difference between the binding of 1F5-B10 to the CD20-negative Jurkat cells in the presence or absence of blocking anti-CD20 antibodies.

### Biodistribution of radioactivity using [$^{211}$At]1F5-B10 anti-CD20 mAb conjugate

Comparative biodistribution studies were performed to assess the abilities of $^{125}$I- and $^{211}$At-labeled 1F5-B10 conjugates to target

**Table 1. Biodistribution of radioactivity (%ID/g tissue) in Ramos xenograft tumors and normal organs 24 hours after injection of radiolabeled antibody conjugates**

|  | [211At]1F5-B10 | [125I]1F5-B10 | [125I]1F5 | [211At]HB8181-B10 | [125I]HB8181-B10 |
|---|---|---|---|---|---|
| Tumor | 9.28 ± 1.85 | 7.53 ± 1.59 | 7.61 ± 2.09 | 3.46 ± 0.58 | 2.87 ± 3.55 |
| Kidney | 6.36 ± 0.54 | 4.24 ± 0.40 | 4.99 ± 0.60 | 5.85 ± 0.49 | 4.4 ± 0.22 |
| Liver | 9.41 ± 0.75 | 4.82 ± 0.38 | 4.71 ± 0.31 | 7.98 ± 0.29 | 5.49 ± .026 |
| Lung | 9.08 ± 1.1 | 7.21 ± 0.89 | 7.06 ± 1.41 | 9.09 ± 0.45 | 7.23 ± 0.44 |
| Blood | 20.23 ± 1.8 | 15.4 ± 0.98 | 19.07 ± 2.65 | 18.67 ± 0.71 | 15.51 ± 0.57 |
| Muscle | 1.31 ± 0.15 | 1.09 ± 0.11 | 1.3 ± 0.27 | 1.26 ± .019 | 1.09 ± 0.06 |

lymphoma xenografts in athymic mice. Tissues were harvested at 1-, 4-, and 24-hour time points, in consideration of the short 7.2-hour half-life of [211]At. Biodistribution studies demonstrated tumor-specific uptake of [211At]1F5-B10 that increased over time with maximum retention 24 hours after injection. Tumor-to-normal organ ratios of absorbed activity were measured in Ramos-tumor–bearing animals (n = 5/group) after receiving [211At]1F5-B10, [125I]1F5-B10, unmodified 1F5 ([125I]1F5), or isotype-matched nonbinding controls ([125I]HB8181-B10, [211At]HB8181-B10). Comparative tumor uptake of activity for the radiolabeled constructs after 24 hours demonstrated near equivalence between all anti-CD20–targeted groups: [211At]1F5-B10 (9.28% ± 1.85%ID/g), [125I]1F5-B10 (7.53% ± 1.59), and [125I]1F5 (7.61% ± 2.09), whereas nonbinding controls had 2.86% ± 0.35%ID/g and 3.45% ± 0.59%ID/g for [125I]HB8181-B10 and [211At]HB8181-B10, respectively. As expected, similar activity from targeted and nontargeted antibodies was observed in nontarget organs. Blood retained a high activity at 24 hours, but the uptake was similar for both radiolabeled 1F5-B10 and HB8181-B10, indicating the nonspecific nature of the finding (Table 1).

### [211]At anti-CD20 therapy in lymphoma xenografts

After biodistribution studies demonstrated the feasibility of administering [211]At-labeled 1F5, we next sought to assess therapeutic efficacy in a subcutaneous Ramos lymphoma xenograft model in athymic mice (n = 10/group) that received 1F5-B10 labeled with [211]At at 3 doses: 12, 16, and 24 μCi. Control mice received either [211At]HB8181-B10 at a dose of 24 μCi (n = 10) or no therapy (n = 10). All mice received syngeneic bone marrow cells 2 days after the treatment dose to ameliorate myelotoxicity. A dose-dependent effect on tumor growth was observed with the highest radiation dose (24 μCi) corresponding to the slowest tumor progression. Similarly, the fastest growth was seen in the untreated control and negative antibody (HB8181) mice. However, the survival rate of the mice receiving the highest treatment dose was only 30% at 40 days after injection (data not shown). Higher doses of radiation (24, 36, and 48 μCi) were explored in the same model; dose-dependent tumor responses were again observed, and the tumor response translated to an improved survival in the [211At]1F5-B10–treated groups as compared with untreated controls (P < .0001 for each [211At]1F5-B10 group compared with untreated controls; Figure 2A). However, despite a promising trend in survival, none of the mice survived beyond 50 days (Figure 2B).

### α-Camera imaging and dosimetry

A heterogeneous intratumoral distribution of α-particles was considered as a possible cause for the suboptimal responses to [211At]1F5-B10 seen in the Ramos lymphoma xenograft model. Digital autoradiography imaging for α-particle detection was used to evaluate the distribution of α-particles in tumors after injection of [211At]1F5-B10. Six athymic nude mice with subcutaneous Ramos tumors received either [211At]1F5-B10 (210 μg; 100 μCi) or control [211At]HB8181-B10

(210 μg; 100 μCi) (n = 3/group). Radioactivity from images of cryosectioned tissues was quantified through calculations based on the linear relationship between pixel intensity and radioactivity (number of decays per unit time). Significant variations in pixel intensity were demonstrated in the Ramos tumors consistent with heterogeneous intratumoral delivery of [211At]1F5-B10. No significant delivery of the nonspecific control [211At]HB8181-B10 was seen (Figure 3).

### [211]At anti-CD20 therapy in a disseminated lymphoma model

Theoretical considerations suggest that the optimal setting for α RIT may be in conditions of isolated disseminated cells and MRD, rather than bulky xenografts. The therapeutic efficacy of conventional RIT using [211]At-labeled 1F5-B10 was therefore evaluated in disseminated
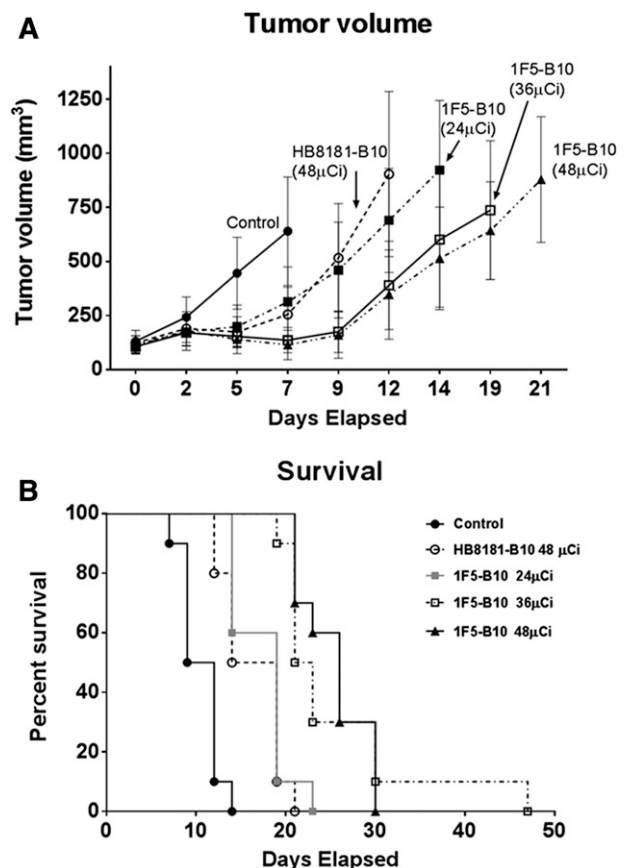


**Figure 2. Analysis of tumor size and cumulative survival of mice bearing Ramos subcutaneous lymphoma xenografts treated with [211]At-labeled 1F5-B10.** (A) Ramos tumor xenografts were serially measured in athymic mice receiving [211At]1F5 (24, 36, or 48 μCi), [211At]HB8181-B10 (48 μCi), or no treatment (control) plotted as mean ± SD. Animals were killed based on the tumor size criteria (16 × 16 × 9 mm). (B) Kaplan-Meier survival curves of the same mice bearing Ramos subcutaneous lymphoma xenografts treated as indicated.

**Figure 3. α-Camera imaging of subcutaneous Ramos xenografts.** Images obtained 28 hours after IV injection of [211At]1F5-B10 (anti-CD20, left) or [211At]HB8181-B10 (control, right), demonstrating specificity of CD20 targeting but heterogeneous dose distributions. Images are color coded to express the intratumoral activity in pCi per voxel (17 × 17 × 16 μm). The white curve represents the activity variation along a line profile placed centrally in each tumor. The white bar (bottom center) indicates 1000 μm.
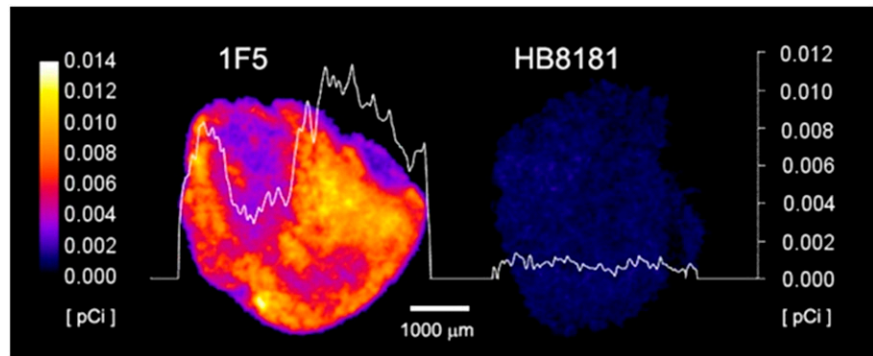


lymphoma mouse models, despite radiosensitivity limitations associated with NOD/SCID mice. These animals uniformly harbor a mutation in the gene for DNA-dependent protein kinase (chromosome 16) resulting in an inability to repair double-strand DNA breaks, which renders them extremely radiosensitive.

A radiotoxicity study was performed to establish the maximal tolerated $^{211}$At radiation doses in this model. Animals (n = 5/group) received 230 μg of 1F5-B10 labeled with either 10 or 20 μCi of $^{211}$At followed by bone marrow rescue ($1 \times 10^7$ bone marrow cells IV from syngeneic donors) 2 days after the treatment dose. This pilot experiment demonstrated that 20 μCi of [211At]1F5-B10 was universally lethal within in 5 days (all animals had stigmata of radiation toxicity including weight loss and petechiae), whereas the 10-μCi dose was well tolerated (Figure 4).

A series of therapy studies were then performed to evaluate the impact of [211At]1F5-B10 on survival in both Ramos (Burkitt) and Granta-519$^{Luc}$ (mantle cell) disseminated lymphoma-bearing mice. In one study, 60 female NOD/SCID mice were IV injected with $1 \times 10^6$ Granta-519$^{Luc}$ tumor cells. Six days later, 2 groups received 7.5 μCi or 15 μCi of [211At]1F5-B10 (n = 10/group). Out of 4 control groups, 2 received either 7.5 μCi or 15 μCi of [211At]HB8181-B10 (n = 10/group), 1 group received a transplant but no therapy (n = 10) and 1 group received unlabeled 1F5-B10 (n = 10). All animals received $1 \times 10^7$ bone marrow cells IV from syngeneic donors 2 days after the treatment dose. Disease progression was followed through serial biweekly BLI. On day 23, BLI revealed significant differences in Granta-519$^{Luc}$ disease burden represented by mean photons/second (p/s) for transplant-only control ($2.58 \times 10^9$ p/s), 7.5-μCi [211At]HB8181-B10 ($2.33 \times 10^9$ p/s), 15-μCi [211At]HB8181-B10 ($2.52 \times 10^8$ p/s), 1F5-B10 alone ($1.14 \times 10^8$ p/s), 7.5-μCi [211At]1F5-B10 ($3.46 \times 10^7$ p/s), and 15-μCi [211At]1F5-B10 ($3.53 \times 10^6$ p/s). Values for 9 out of 10 animals in the 15-μCi [211At]1F5-B10 group were not statistically different from background values obtained from an age-matched cohort of non–disease-bearing mice ($1.12 \times 10^6$ p/s) (Figure 5A,C). By day 47, 100% of the mice in the control group receiving 7.5-μCi [211At] HB8181-B10, 80% receiving bone marrow rescue alone, and and 60% of mice in the 15-μCi [211At]HB8181-B10 group had died of progressive disease, whereas 100% of the mice receiving 7.5 or 15 μCi of [211At]1F5-B10 remained alive. In the group receiving 1F5-B10 alone without radiation, 90% of the animals were also alive at day 47; however, BLI on day 57 demonstrated that all surviving animals in this group had a significant disease burden consistent with only a modest antitumor effect attributable to the 1F5 mAb (Figure 5B). By day 75, all [211At]HB8181-B10 control animals were dead, whereas 80% of the 15-μCi [211At]HB8181-B10 group and 30% of the 7.5-μCi [211At]1F5-B10 group remained alive; the median overall survival was significantly longer in the experimental

treatment groups ([211At]1F5-B10) compared with the control groups ([211At]HB8181-B10 or bone marrow rescue only; $P < .001$ for both) (Figure 6). BLI performed on day 132 revealed that 70% of animals in the 15-μCi [211At]1F5-B10 group continued to have no detectable disease.

No early deaths attributable to radiation toxicity were seen in this study. Mice were weighed daily, and at a time point when all mice in all study groups remained alive after treatment (day 20), the animals had average body weights of $102\% \pm 3.8\%$ (transplant alone), $101\% \pm 4.2\%$ (1F5-B10 control), $100\% \pm 4.3\%$ (7.5-μCi [211At]HB8181-B10), $96.5\% \pm 3.9\%$ (15-μCi [211At]HB8181-B10), $98.6\% \pm 3.8\%$ (7.5-μCi [211At]1F5-B10), and $93.6\% \pm 5.8\%$ (15-μCi [211At]1F5-B10). An additional series of studies following the same design was performed using disseminated Ramos lymphoma, and similar results were demonstrated (at day 80): 80% survival for 15-μCi [211At]1F5-B10–treated animals, 70% for animals treated with 10-μCi [211At]1F5-B10, 10% in transplant-only controls, and no surviving animals in the 10- or 15-μCi [211At]HB8181-B10 control groups.

To evaluate therapy-associated toxicity, terminal bleeds were performed on all surviving animals after 130 days to evaluate renal, hepatic, and bone marrow function. Values were compared with published normal values for NOD/SCID mice.[32] Among the 7 surviving animals treated with 15-μCi [211At]1F5-B10, there was no evidence of impaired renal or hepatic function. Bone marrow function was also preserved with no decrement in leukocyte or platelet counts. Mild anemia was observed in comparison with
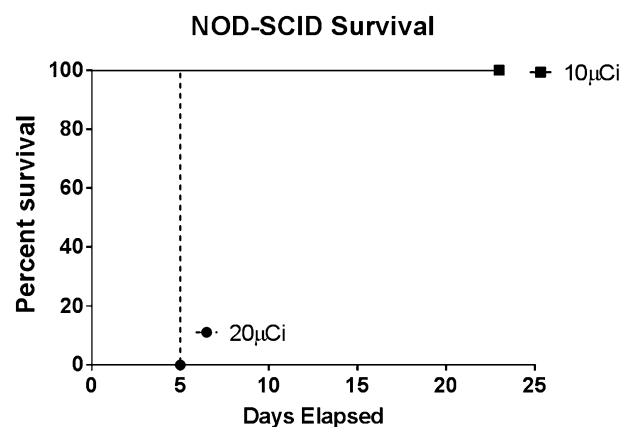


**Figure 4. $^{211}$At radiosensitivity of NOD/SCID mice.** Non-tumor–bearing NOD/SCID mice (n = 5/group) received 230 μg of 1F5-B10 labeled with either 10 or 20 μCi of $^{211}$At followed by bone marrow rescue ($1 \times 10^7$ bone marrow cells IV from syngeneic donors) 2 days after treatment. The Kaplan-Meier survival curves demonstrates that 20-μCi [211At]1F5-B10 was universally lethal within in 5 days, whereas the 10-μCi dose was well tolerated.
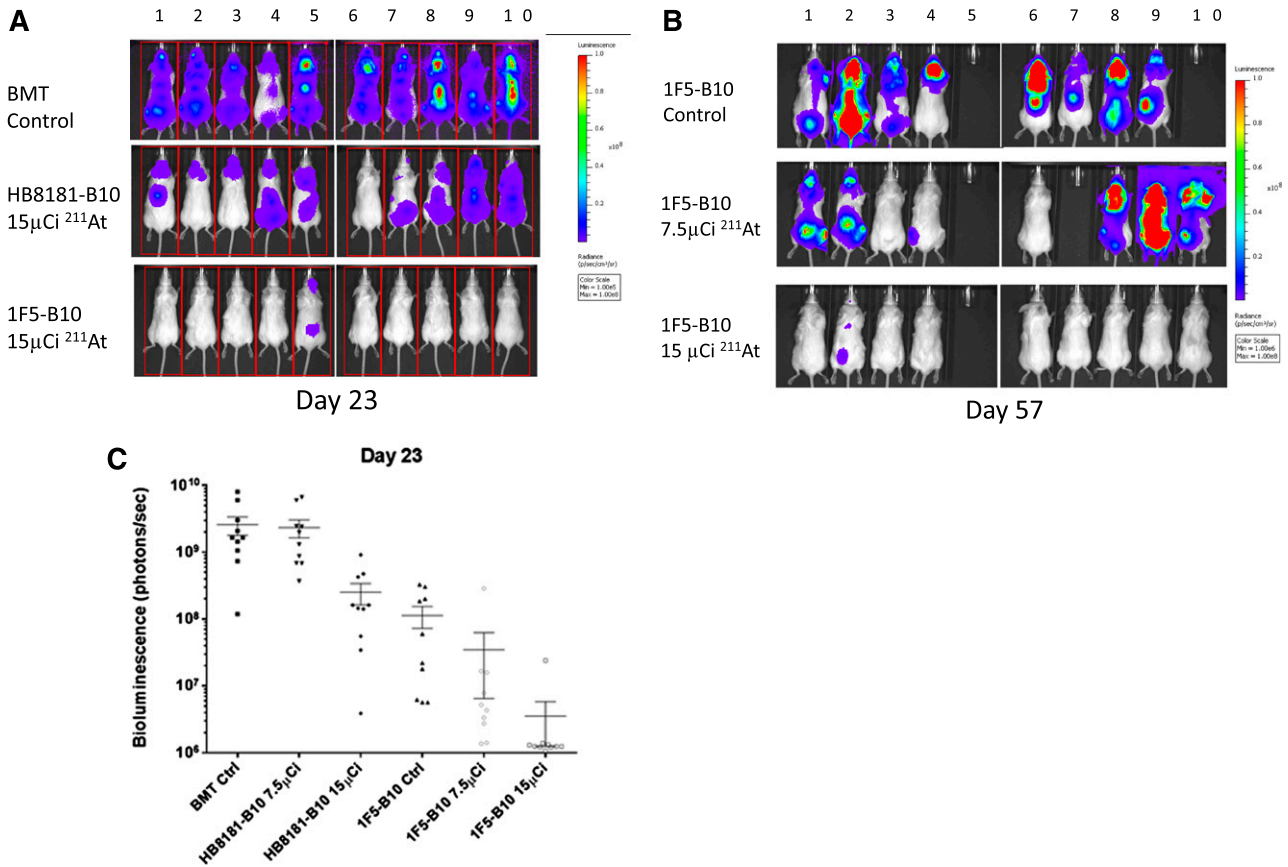
Figure 5. Efficacy of [211]At-B10-1F5 in an MRD model. Mice were inoculated via IV injection of Granta 519[Luc] cells ($1 \times 10^6$) and monitored for tumor progression by BLI twice weekly for the duration of the study. On day 6, animals received 7.5 or 15 μCi of [211]At-labeled 1F5-B10 (anti-CD20 mAb) or HB8181-B10 (nonbinding mAb control) or 1F5-B10 antibody alone or no therapy. All animals received stem cell rescue, either 2 days after the radiation dose (1F5-B10 or HB8181-B10 groups) or at the same time point without radiation (bone marrow transplant [BMT] control group). (A) Whole-body ventral BLI images on day 23 demonstrate diffuse signal corresponding with disease involvement in both control groups, with only 1 mouse demonstrating measurable disease in the 15-μCi anti-CD20–treated group. (B) Day-57 imaging of all surviving animals. (C) BLI plot demonstrating the mean ± standard error of the mean p/s for each group. The imaging data were normalized to the same scale for each figure.

normal controls; however, control animals did not undergo stem cell rescue (Table 2).

## Discussion

Evidence that the efficacy of α-particle RIT is a function of tumor cell accessibility is compellingly demonstrated by differences in response to [211]At]1F5-B10 therapy seen in the 2 disease models described in this article. When uniform target distribution is not possible, tumor cell escape represents the likely cause of disease relapse after RIT. In contrast, our MRD model results suggest uniform delivery of [211]At]1F5-B10 to tumor cells that results in disease eradication. In animals with subcutaneous lymphoma xenografts treated with high doses of [211]At]1F5-B10 (48 μCi), only modest attenuation in tumor growth and slightly longer survival were demonstrated (Figure 2B). In sharp contrast, when the same tumor cell lines were studied in a disseminated model consisting of isolated single tumor cells or small tumor cell clusters, a 15-μCi dose resulted in complete eradication of disease in 70% of animals (Figure 6). Tumor growth in untreated control animals was aggressive and uniformly lethal in both models. Strikingly, 100% of the treated animals in the subcutaneous tumor model succumbed to disease (or radiation toxicity) by day 47, whereas in the disseminated model, 100% of

mice receiving either 7.5- or 15-μCi doses of [211]At]1F5-B10 remained alive on day 47 despite receiving a radiation dose that was less than one-third of the highest dose administered in the subcutaneous tumor experiments (48 μCi).

Our cell-binding results both demonstrate the stability of the α-emitter–labeled mAb-B10 conjugate and confirm the comparable binding characteristics of unmodified 1F5 mAb and 1F5-B10 conjugate (Figure 1). We also report equivalent tumor uptake and tissue biodistributions with [125I]1F5, [125I]1F5-B10, and [211]At]1F5-B10. Two important conclusions may be drawn from these data: first, the *closo*-decaborate(2-) (B10-NCS) conjugate does not impair the binding function of the parent anti-CD20 molecule; and second, the astatination process does not impair 1F5-binding affinity.

Our group and others have demonstrated that α-particle RIT may be superior to β-particle–based therapy in micrometastatic disease, and the promise of this approach in MRD has also been suggested.[33-37] Mathematical modeling has demonstrated that tumors with dimensions of <1 mm are relatively resistant to β-emitting radionuclides (^{90}Y) because only a very small fraction of the disintegration energy is deposited into the actual tumor mass.[38] For example, when meta-[^{131}I] iodobenzylguanidine was evaluated to assess response in neuroblastoma spheroids of 2 different diameters (250 and 400 μm), regrowth delay was shorter and cure rates were lower with the smaller spheroid.[38] In contrast, α-particles deposit ≥500 times more energy per unit length

Figure 6. Kaplan-Meier survival curves of mice bearing disseminated lymphoma. Groups of 10 mice bearing disseminated lymphoma after IV Granta-519[Luc] (MCL) injections 6 days before treatment. Mice in the treatment groups were treated with 7.5 or 15 μCi of radiation via 1F5-B10 (anti-CD20), HB8181-B10 (non-binding control), or 1F5-B10 (unlabeled mAb control). All animals received stem cell rescue either 2 days after the radiation dose (1F5-B10 or HB8181-B10 groups) or at the same time point without radiation (BMT control group).
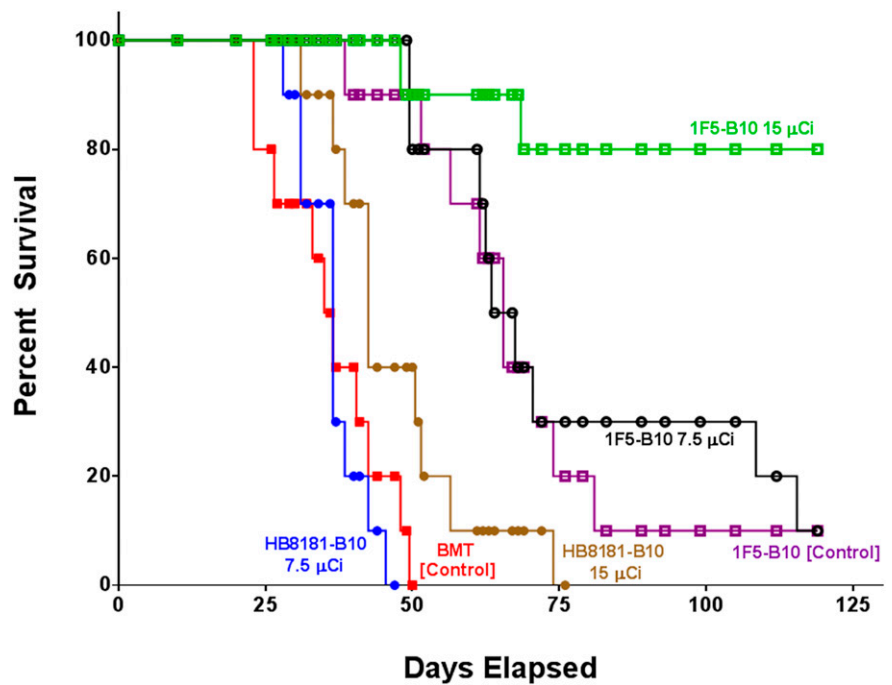
than β-emitters,[39] and as few as 1 to 5 α-particle emissions can be sufficient to cause irreparable DNA damage and cell death.[40,41] These physical characteristics of α-emitters provide a basis for understanding the differences between results in our xenograft and MRD models. When sufficient radiation doses are achieved through tumor pretargeting, β-emitter RIT has been shown to effectively eliminate bulky subcutaneous xenograft tumors in mice.[42,43] In these conglomerate tumor masses, β-emitters can mitigate heterogenous target tissue distribution of the radiolabeled antibody through crossfire irradiation from surrounding cells, whereas the short range of α-emitters is clearly less well suited to this situation. Through α-camera imaging performed on excised subcutaneous tumors 28 hours after [211At]1F5-B10 injection, we demonstrate intratumoral heterogeneity predictive of the modest responses seen in our subcutaneous lymphoma xenograft therapy studies. This finding suggests an explanation for why high-injected activities of [211At]1F5-B10 proved incapable of tumor eradication in the subcutaneous model while lower activity was effective in the MRD model where α-emitting radionuclides can achieve the requisite tumor cell proximity, enabling delivery of their energy dose to the targets.[39]

We selected the disseminated mouse lymphoma model to recapitulate MRD because the absence of grossly detectable disease by BLI at the time point when the [211At]1F5-B10 was administered, followed by subsequent identification of measurable disease in all control animals over time, reflects the same pattern as progression from MRD to fulminant disease in clinical settings. The profound radiosensitivity of the NOD/SCID host necessary for this model represents a limitation, however, as it significantly limits radiation dose escalation (Figure 4). Despite this limitation, 70% of animals treated at the highest tolerable dose evaluated (15 μCi) were cured, raising the possibility that absent the exquisite radiation sensitivity unique to the model required to mimic MRD, even higher rates of response and cure may be achievable.

In the NOD/SCID MRD model, a mild but nevertheless statistically significant antitumor effect attributable to nonspecific radiation was seen in animals receiving 15-μCi [211At]HB8181-B10 based on BLI measuring p/s performed on day 23 (transplant-only control [2.58 × 10⁹ p/s]; 15-μCi [211At]HB8181-B10 [2.52 × 10⁸ p/s]; $P = .02$); however, the effect was transient, and all animals in this group died of disease progression by day 75 (Figure 6). Moreover, day-23 BLI demonstrated a significantly larger tumor burden in these nontargeted [211At]HB8181-B10 (15-μCi) control mice as compared with those receiving 15 μCi of targeted anti-CD20 [211At]1F5-B10 (3.53 × 10⁶ p/s) ($P = .02$). Anti-CD20 mAb administered as a single agent without radiation also had a mild independent antitumor effect based on day-23 BLI ($P = .01$); however, the impact was also transient, with all animals in the 1F5-B10 alone (no radiation control) group demonstrating widespread disease on day 57 (Figure 5B).

Overall, [211At]1F5-B10 was well tolerated. Unlike ²¹³Bi, which generates nephrotoxicity in preclinical lymphoma models,[44] no late nephrotoxicity or hepatotoxicity was seen in our studies, likely reflecting superior conjugate stability after ²¹¹At radiolabeling.[45] In addition, ²¹¹At does not generate toxic decay products.[46] In future clinical trials, these favorable properties could also limit exposure risk to caregivers (health care providers and patient families).

In conclusion, although the number of highly active therapies available for the treatment of relapsed indolent lymphoma and MCL has increased dramatically over the past 2 decades, these diseases remain incurable. Unlike other therapies, α-particle–based

**Table 2. White blood cell, hematocrit, platelet, creatinine, and alanine aminotransferase values obtained from [²¹¹At]1F5-B10 (15 μCi) at terminal bleed after 130 days and matched normal values**

| | WBC (×10⁹/L) | HCT (%) | Platelets (×10⁹/L) | Creatinine (mg/dL) | ALT (U/L) |
|---|---|---|---|---|---|
| [²¹¹At]1F5-B10 (15 μCi; n = 7) | 2.4 ± 1.14 | 41 ± 4.3 | 1566 ± 480 | 0.2 ± .07 | 68 ± 27 |
| Normal values[32] | 2.0 ± 0.3 | 50 ± 1.0 | 724 ± 52 | 0.4 ± 0 | 69 ± 23 |

ALT, alanine aminotransferase; HCT, hematocrit; WBC, white blood cell.

RIT is not cell-cycle specific and can selectively kill all cells whose nuclei are within its short path length. As a result, $[^{211}At]1F5$-B10 has the potential to overcome treatment-resistant MRD lymphoma cell clones that have evaded other forms of therapy. Our studies demonstrate that $\alpha$-particle RIT may hold particular promise as a means to achieve MRD elimination, and results support further evaluation in clinical trials.

## Acknowledgments

## Authorship

Correspondence: Damian J. Green, Clinical Research Division, Fred Hutchinson Cancer Research Center, 1100 Fairview Ave North, MS: D3-190, Seattle, WA 98109; e-mail: dgreen@fhcrc.org.

## References

1. Wang ML, Rule S, Martin P, et al. Targeting BTK with ibrutinib in relapsed or refractory mantle-cell lymphoma. N Engl J Med. 2013;369(6):507-516.

2. Fisher RI, Dahlberg S, Nathwani BN, Banks PM, Miller TP, Grogan TM. A clinical analysis of two indolent lymphoma entities: mantle cell lymphoma and marginal zone lymphoma (including the mucosa-associated lymphoid tissue and monocytoid B-cell subcategories): a Southwest Oncology Group study. Blood. 1995;85(4): 1075-1082.

3. Dreyling M, Hiddemann W; European MCL Network. Current treatment standards and emerging strategies in mantle cell lymphoma. Hematology Am Soc Hematol Educ Program. 2009;2009(1):542-551.

4. Gribben JG, Neuberg D, Freedman AS, et al. Detection by polymerase chain reaction of residual cells with the bcl-2 translocation is associated with increased risk of relapse after autologous bone marrow transplantation for B-cell lymphoma. Blood. 1993;81(12):3449-3457.

5. Gribben JG, Neuberg D, Barber M, et al. Detection of residual lymphoma cells by polymerase chain reaction in peripheral blood is significantly less predictive for relapse than detection in bone marrow. Blood. 1994;83(12): 3800-3807.

6. Hirt C, Schüler F, Kiefer T, et al. Rapid and sustained clearance of circulating lymphoma cells after chemotherapy plus rituximab: clinical significance of quantitative t(14;18) PCR monitoring in advanced stage follicular lymphoma patients. Br J Haematol. 2008;141(5):631-640.

7. Kolstad A, Laurell A, Jerkeman M, et al; Nordic Lymphoma Group. Nordic MCL3 study: 90Y-ibritumomab-tiuxetan added to BEAM/C in non-CR patients before transplant in mantle cell lymphoma. Blood. 2014;123(19):2953-2959.

8. Pott C, Schrader C, Gesk S, et al. Quantitative assessment of molecular remission after high-dose therapy with autologous stem cell transplantation predicts long-term remission in mantle cell lymphoma. Blood. 2006;107(6): 2271-2278.

9. Press OW, Eary JF, Appelbaum FR, et al. Radiolabeled-antibody therapy of B-cell lymphoma with autologous bone marrow support. N Engl J Med. 1993;329(17):1219-1224.

10. Press OW, Eary JF, Appelbaum FR, et al. Phase II trial of 131I-B1 (anti-CD20) antibody

therapy with autologous stem cell transplantation for relapsed B cell lymphomas. Lancet. 1995; 346(8971):336-340.

11. Goldenberg DM, Sharkey RM. Radioimmunotherapy of non-Hodgkin's lymphoma revisited. J Nucl Med. 2005;46(2): 383-384.

12. Kaminski MS, Tuck M, Estes J, et al. 131I-tositumomab therapy as initial treatment for follicular lymphoma. N Engl J Med. 2005;352(5): 441-449.

13. Kaminski MS, Tuck M, Regan D, Kison P, Wahl RL. High response rates and durable remissions in patients with previously untreated, advanced-stage, follicular lymphoma treated with toistumomab and Iodine I-131 tositumomab (Bexxar®) [abstract]. Blood. 2002;100(11):356a. Abstract 1381.

14. Wiseman GA, Witzig TE. Yttrium-90 (90Y) ibritumomab tiuxetan (Zevalin) induces long-term durable responses in patients with relapsed or refractory B-Cell non-Hodgkin's lymphoma. Cancer Biother Radiopharm. 2005;20(2):185-188.

15. Witzig TE, Gordon LI, Cabanillas F, et al. Randomized controlled trial of yttrium-90-labeled ibritumomab tiuxetan radioimmunotherapy versus rituximab immunotherapy for patients with relapsed or refractory low-grade, follicular, or transformed B-cell non-Hodgkin's lymphoma. J Clin Oncol. 2002;20(10):2453-2463.

16. Vose JM, Bierman PJ, Enke C, et al. Phase I trial of iodine-131 tositumomab with high-dose chemotherapy and autologous stem-cell transplantation for relapsed non-Hodgkin's lymphoma. J Clin Oncol. 2005;23(3):461-467.

17. Witzig TE, Fishkin P, Gordon LI, et al. Treatment recommendations for radioimmunotherapy in follicular lymphoma: a consensus conference report. Leuk Lymphoma. 2011;52(7):1188-1199.

18. Gopal AK, Rajendran JG, Petersdorf SH, et al. High-dose chemo-radioimmunotherapy with autologous stem cell support for relapsed mantle cell lymphoma. Blood. 2002;99(9):3158-3162.

19. Fisher RI, Kaminski MS, Wahl RL, et al. Tositumomab and iodine-131 tositumomab produces durable complete remissions in a subset of heavily pretreated patients with low-grade and transformed non-Hodgkin's lymphomas. J Clin Oncol. 2005;23(30):7565-7573.

20. Apostolidis J, Gupta RK, Grenzelias D, et al. High-dose therapy with autologous bone marrow

support as consolidation of remission in follicular lymphoma: long-term clinical and molecular follow-up. J Clin Oncol. 2000;18(3):527-536.

21. Vose JM, Wahl RL, Saleh M, et al. Multicenter phase II study of iodine-131 tositumomab for chemotherapy-relapsed/refractory low-grade and transformed low-grade B-cell non-Hodgkin's lymphomas. J Clin Oncol. 2000;18(6):1316-1323.

22. Witzig TE, Flinn IW, Gordon LI, et al. Treatment with ibritumomab tiuxetan radioimmunotherapy in patients with rituximab-refractory follicular non-Hodgkin's lymphoma. J Clin Oncol. 2002;20(15): 3262-3269.

23. Press OW, Eary JF, Gooley T, et al. A phase I/II trial of iodine-131-tositumomab (anti-CD20), etoposide, cyclophosphamide, and autologous stem cell transplantation for relapsed B-cell lymphomas. Blood. 2000;96(9):2934-2942.

24. Winter JN, Inwards DJ, Spies S, et al. Yttrium-90 ibritumomab tiuxetan doses calculated to deliver up to 15 Gy to critical organs may be safely combined with high-dose BEAM and autologous transplantation in relapsed or refractory B-cell non-Hodgkin's lymphoma. J Clin Oncol. 2009; 27(10):1653-1659.

25. Wilbur DS, Chyan MK, Hamlin DK, Perry MA. Reagents for astatination of biomolecules. 3. Comparison of closo-decaborate(2-) and closo-dodecaborate(2-) moieties as reactive groups for labeling with astatine-211. Bioconjug Chem. 2009;20(3):591-602.

26. Wilbur DS, Chyan MK, Nakamae H, et al. Reagents for astatination of biomolecules. 6. An intact antibody conjugated with a maleimido-closo-decaborate(2-) reagent via sulfhydryl groups had considerably higher kidney concentrations than the same antibody conjugated with an isothiocyanato-closo-decaborate(2-) reagent via lysine amines. Bioconjug Chem. 2012;23(3):409-420.

27. Orozco JJ, Bäck T, Kenoyer A, et al. Anti-CD45 radioimmunotherapy using (211)At with bone marrow transplantation prolongs survival in a disseminated murine leukemia model. Blood. 2013;121(18):3759-3767.

28. Wilbur DS, Vessella RL, Stray JE, Goffe DK, Blouke KA, Atcher RW. Preparation and evaluation of para-[211At]astatobenzoyl labeled anti-renal cell carcinoma antibody A6H F(ab')2. In vivo distribution comparison with para-[125I]iodobenzoyl labeled A6H F(ab')2. Nucl Med Biol. 1993;20(8):917-927.

29. Bäck T, Jacobsson L. The alpha-camera: a quantitative digital autoradiography technique using a charge-coupled device for ex vivo high-resolution bioimaging of alpha-particles. *J Nucl Med.* 2010;51(10):1616-1623.

30. Chouin N, Lindegren S, Frost SH, et al. Ex vivo activity quantification in micrometastases at the cellular scale using the α-camera technique. *J Nucl Med.* 2013;54(8):1347-1353.

31. Robinson MK, Shaller C, Garmestani K, et al. Effective treatment of established human breast tumor xenografts in immunodeficient mice with a single dose of the alpha-emitting radioisotope astatine-211 conjugated to anti-HER2/neu diabodies. *Clin Cancer Res.* 2008;14(3):875-882.

32. Janvier Labs. Technical Sheet: CB17-SCID immunodeficient mouse. http://www.janvier-labs.com/tl_files/_media/images/FICHE_RESEARCH_MODEL_CB17SCID.pdf. Accessed November 11, 2014.

33. Park SI, Shenoi J, Pagel JM, et al. Conventional and pretargeted radioimmunotherapy using bismuth-213 to target and treat non-Hodgkin lymphomas expressing CD20: a preclinical model toward optimal consolidation therapy to eradicate minimal residual disease. *Blood.* 2010;116(20):4231-4239.

34. Zalutsky MR. Targeted alpha-particle therapy of microscopic disease: Providing a further rationale for clinical investigation. *J Nucl Med.* 2006;47(8):1238-1240.

35. Song EY, Qu CF, Rizvi SM, et al. Bismuth-213 radioimmunotherapy with C595 anti-MUC1 monoclonal antibody in an ovarian cancer ascites model. *Cancer Biol Ther.* 2008;7(1):76-80.

36. Song YJ, Qu CF, Rizvi SM, et al. Cytotoxicity of PAI2, C595 and Herceptin vectors labeled with the alpha-emitting radioisotope Bismuth-213 for ovarian cancer cell monolayers and clusters. *Cancer Lett.* 2006;234(2):176-183.

37. Chouin N, Lindegren S, Jensen H, Albertsson P, Bäck T. Quantification of activity by alpha-camera imaging and small-scale dosimetry within ovarian carcinoma micrometastases treated with targeted alpha therapy. *Q J Nucl Med Mol Imaging.* 2012;56(6):487-495.

38. O'Donoghue JA, Bardiès M, Wheldon TE. Relationships between tumor size and curability for uniformly targeted therapy with beta-emitting radionuclides. *J Nucl Med.* 1995;36(10):1902-1909.

39. Baidoo KE, Yong K, Brechbiel MW. Molecular pathways: targeted α-particle radiation therapy. *Clin Cancer Res.* 2013;19(3):530-537.

40. Kennel SJ, Stabin M, Roeske JC, et al. Radiotoxicity of bismuth-213 bound to membranes of monolayer and spheroid cultures of tumor cells. *Radiat Res.* 1999;151(3):244-256.

41. McDevitt MR, Sgouros G, Finn RD, et al. Radioimmunotherapy with alpha-emitting nuclides. *Eur J Nucl Med.* 1998;25(9):1341-1351.

42. Press OW, Corcoran M, Subbiah K, et al. A comparative evaluation of conventional and pretargeted radioimmunotherapy of CD20-expressing lymphoma xenografts. *Blood.* 2001;98(8):2535-2543.

43. Green DJ, Orgun NN, Jones JC, et al. A preclinical model of CD38-pretargeted radioimmunotherapy for plasma cell malignancies. *Cancer Res.* 2014;74(4):1179-1189.

44. Zalutsky MR, Pozzi OR. Radioimmunotherapy with alpha-particle emitting radionuclides. *Q J Nucl Med Mol Imaging.* 2004;48(4):289-296.

45. Wilbur DS. [211At]Astatine-labeled compound stability: issues with released [211At]astatide and development of labeling reagents to increase stability. *Curr Radiopharm.* 2008;1(3):144-176.

46. Vaidyanathan G, Zalutsky MR. Astatine radiopharmaceuticals: prospects and problems. *Curr Radiopharm.* 2008;1(3):177.